Journal of Atomic and Molecular Sciences

Global Science Press

ISSN 2075-1303

Theoretical Study on Chemospecificity of $CF_3SO_3CF_2CF_3 + F^-$ Reactions

Received Oct. 22, 2017,
Accepted Dec. 12, 2017,

DOI: 10.4208/jams.102217.121217a

http://www.global-sci.org/jams/

Li Guo[a], Yulong Xu[a,]*

Abstract. DFT and ab initio methods are used to investigate why the reaction, $C(1)F_3S(2)O_2O(3)C(4)F_2C(5)F_3 + F^-$, results in the S-O cleavage chemospecifically. Three S_N2 channels, i.e. S-O cleavage and back- and front-side of C-O scission are predicted to occur. The F(11)and F(12) atoms of the $C(4)F_2$ group play the multiple roles in three paths. Multi-membered rings are formed in C-O rupture mechanisms due to the neighboring effect. The rate of S-O scission reaction is 10^{31} time as large as the rates of C-O rupture reactions. It is the combination of the irreversibility and the huge rate ratios to determine that S-O cleavage is chemospecific. This conclusion agrees well with the experimental results.

1. Introduction

Since the 1930s, halonium ions have been known to be a great source for unique synthetic pathways and insight into reaction mechanisms[1]. Organofluorine compounds have found widespread applications in diverse areas such as polymers, liquid crystals, and agricultural and medicinal chemistry[2-6]. Partial or full fluorination provides distinctive physicochemical properties to an organic molecule that can be attributed to the special properties of the carbonfluorine (C-F) bond[6]. Fluorine is the most electronegative (electron-attracting) element of the periodic table, so the C-F bond is highly polarized. Because of its small size and its high electronegativity, fluorine's electrons are poorly polarizable, and organofluorine compounds generally interact with other atoms or molecules only through rather weak electrostatic interactions[7,8]. The S_N2 nucleophilic substitution reaction is one of the most extensively studied chemical reactions in solution.

Hydrolysis of sulfonic ester RSO_2OR' is a S_N2 reaction[9], and the R'-O cleavage is much more likely than S-O cleavage when R' is alkyl. On the other hand, the S-O bond is much more likely to cleave when R' is aryl[9,10]. Such chemospecificity has also been found in the nucleophilic substitutions at perfluoro- and polyfluoro-sulfonic ester. In reaction (I), as shown by the experiments and theoretical study[11a, 11c], the nucleophile, such as F^-, attacks $RFSO_3CH_2R'F$ at the α-carbon atom, leading to the C-O cleavage exclusively. But reaction (Ⅱ) leads to the S-O cleavage solely[11b]. Such chemospecificity was ascribed to the screen effect and the electron repulsion between F^- and two fluorine atoms on the α-carbon atom. It is due to reaction (III) that reaction (II) can lead, specifically, to the S-O cleavage. Therefore, it is necessary to theoretically understand the chemospecificity of reactions (I) and (II) as well as to detail the roles of the α-group and β-group. In this paper, the DFT and ab initio methods (HF and MP2) are used to investigate reaction (II), and the theoretical research on the reaction (I) had been reported in this journal.

$$R_FSO_3CH_2R'_F + Nu^- \xrightarrow[\text{Cleavage}]{\text{C-O}} R_FSO_3^- + NuCH_2R'_F \quad (I)$$

$$R_FSO_3CF_2R'_F + Nu^- \xrightarrow[\text{Cleavage}]{\text{S-O}} R_FSO_2Nu + {}^-OCF_2R'_F \quad (II)$$

$$\longrightarrow R'_FCOF + F^- \quad (III)$$

There are three ways for F^- to attack $C(1)F_3S(2)O_2O(3)C(4)F_2C(5)F_3$ (PFS): (i) at the S atom from the backside of the O(3) atom, denoted as $S_N2(S)$; (ii) at the α-C atom from the backside of the O(3) atom(the S_N2 (C-B) mechanism); (iii) at the α-C atom from the frontside of the O(3) atom, denoted as S_N2(C-F). As the strongly electron-withdrawing group, two F atoms in the $C(4)F_2$ group play the multiple roles in three reaction paths. Their roles in determining chemospecificity of the reaction are particularly interesting. The multiple electrophilic centers are involved in the C-O scission reactions. At last, the kinetic analysis is performed.

2. Calculation Method

All computations are done using the Gaussian 09 program package[12]. The reactants, products, intermediates and transition states are optimized using B3LYP at 6-31+G* level. The harmonic vibration frequencies are calculated with the same method, and each transition state is characterized by one imaginary frequency. Afterwards, the IRC (intrinsic reaction coordinate) method[13] is used to track minimum energy path from transition state to the corresponding local minima.

In each of three S_{N2} reactions, the charge, which is located to F^- before reaction, becomes dispersed over a somewhat larger area in the reactant complex and transition state (Figure 2.1). The solvent effects on the reaction are examined using the SCRF method [14], but those are so slight that discussion will not be presented in this work.

[a.] School of Chemistry and Pharmaceutical Engineering, Qilu University of Technology(Shandong Academy of Sciences), Jinan, Shandong 250353, China
[b.] School of science, Qilu University of Technology(Shandong Academy of Sciences), Jinan, Shandong 250353, China
*Corresponding author. Email:yulongxu@163.com

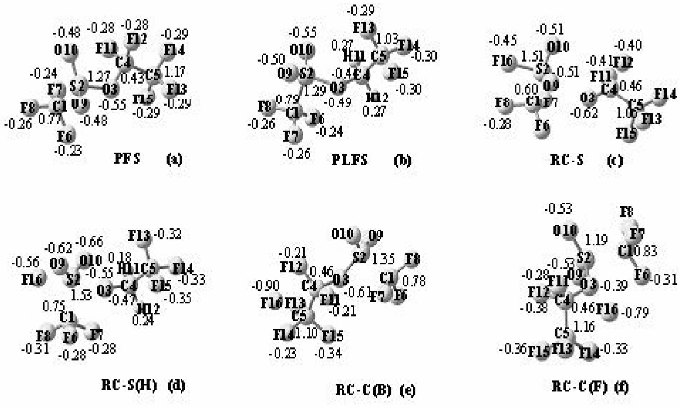

Figure 2.1: The Mulliken atomic charges obtained at B3LYP/6-31+G* level (PFS refers to a perfluoroethylsulfonate $CF_3SO_3CF_2CF_3$ and PLFS denotes a polyfluoroethylsulfonate $CF_3SO_3CH_2CF_3$.)

3. Results and discussion

3.1 The C-O Cleavage Mechanism.

As early indicated by March [9a], it is impossible for the frontside S_N2 mechanism to be observed. Recently, however, some experimental and theoretical chemists indicated that the frontside S_N2 mechanism is possible[9b,15]. In this work, it seems to be a possible way for F^- to attack PFS at the C(4) atom from the front side of the O(3) atom besides the well-know backside S_N2 mechanism.

3.1.1 The Backside S_N2 Mechanism.

In this mechanism, reactant complex, transition and product complex are denoted as RC-C(B), TS-C(B) and PC-C(B) respectively. RC-C(B) can be obtained from geometry optimization using B3LYP/6-31+G*, but it is almost impossible for the DFT method to locate a reasonable TS-C(B) although various efforts have been made. Fortunately, HF and MP2 methods are productive.

As shown in Figure 3.1.1, the conformations of RC-C(B), TS-C(B) and PC-C(B), obtained from the MP2 and HF/6-31+G*, are similar, but their geometrical data, such as the distances $r_{16,4}$ and $r_{16,5}$, the dihedral angle F(13)-C(5)-C(4)-F(16) as well as the bond angles ∠F(16)-C(5)-F(13) and ∠F(16)-C(4)-O(3), are obviously different from the corresponding those obtained from B3LYP/6-31+G*. For example, in RC-C(B), the distances $r_{16,5} \approx r_{16,4}$ (about 2.5 Å), and $r_{5,13} > r_{5,15} \approx r_{5,14}$ (HF and MP2). But the distances, $r_{16,4}$ (2.778 Å) < $r_{16,5}$ (3.130 Å) at B3LYP/631+G* level (the symbol "$r_{m,n}$" denotes the distance between the *m*th and *n*th atoms).

It will be found that the distance $r_{16,4}$ in the S_N2(C-B) mechanism is the longest of three possible mechanisms as far as the distance between F^- and the reaction center is concerned. As shown by the atomic charges (-0.28) of the F(11) and F(12) atoms (Figure 2.1a), the shielding effect, exerted by the F(11) and F(12) atoms, is a resistance to F^- attacking PFS at the atom C(4) from the backside of the O(3) atom, and DFT method is more sensitive to the shielding effect[16]. On the contrary, the group C(5)F3, as a neighbor of the reaction center C(4), may play a role in stabilizing RC-C(B) (neighboring effect) according to the dihedral angle F(13)-C(5)-C(4)-F(16) as well as to ∠F(16)-C(5)-F(13) and ∠F(16)-C(4)-O(3) in RC-B. In appearance, F^- attacks PFS at the C(4) and C(5) atoms, and a three-membered ring, F(16)-C(4)-C(5)-F(16), is formed in RC-C(B) and TS-C(B). In Figures 3.1.1a and 3.1.1b, for example, the dihedral angles F(13)-C(5)-C(4)-F(16) are 179.7° (HF/6-31+G*) and 179.8° (MP2/6-31+G*), ∠F(16)-C(4)-O(3) and ∠F(16)-C(5)-F(13) are: 177.7° and 179.2° (HF), 176.0° and 177.9° (MP2). Those mean that the F(16), C(4), C(5), O(3) and F(13) atoms in RC-C(B) are almost coplanar at HF and MP2/6-31+G* levels. In the meantime, the bond length $r_{5,13}$ is always longer than those $r_{5,14}$ and $r_{5,15}$. In the geometry obtained from DFT, the distance $r_{16,4}$ is the longest of three geometries of RC-B (Figures 3.1.1a~3.1.1c), and it is so long that the neighboring effect is weaker than that in each of two other geometries (Figures 3.1.1a and 3.1.1b). Correspondingly, $r_{16,4}$ = 2.778 Å < $r_{16,5}$ = 3.130 Å, ∠F(16)-C(5)-F(13) = 121.1° and the dihedral angle F(13)-C(5)-C(4)-F(16) = 116.5° (Figure 3.1.1c). The distance $r_{4,3}$ is getting longer while *r*16,4, is being shortened with the attack of F−, and a transition state is reached. In the meantime, the dihedral angle C(5)-C(4)-F(11)-F(12) is enlarged from about 130º to about 150° (Figures 3.1.1d and 3.1.1e), and $r_{16,4} < r_{16,5}$. In the vibrational model characterized by an imaginary frequency 560.7 cm^{-1}, as shown by the arrows in Figure 2f, the C(5)-C(4) bond looks like a pendulum, and the positions of the C(5), F(11) and F(12) atoms keep unchanged while the C(4)-F(16) and C(4)-O(3) bonds stretch. At last, the PC-C(B) is formed, and meanwhile the values of the dihedral angle C(5)-C(4)-F(11)-F(12) are -122.8° (MP2/6-31+G*), -122.6° (HF/6-31+G*) and –123.0° (B3LYP/6-31+G*). The configuration of molecule is inverted in PC-C(B) (Figures 3.1.1g~3.1.1i).

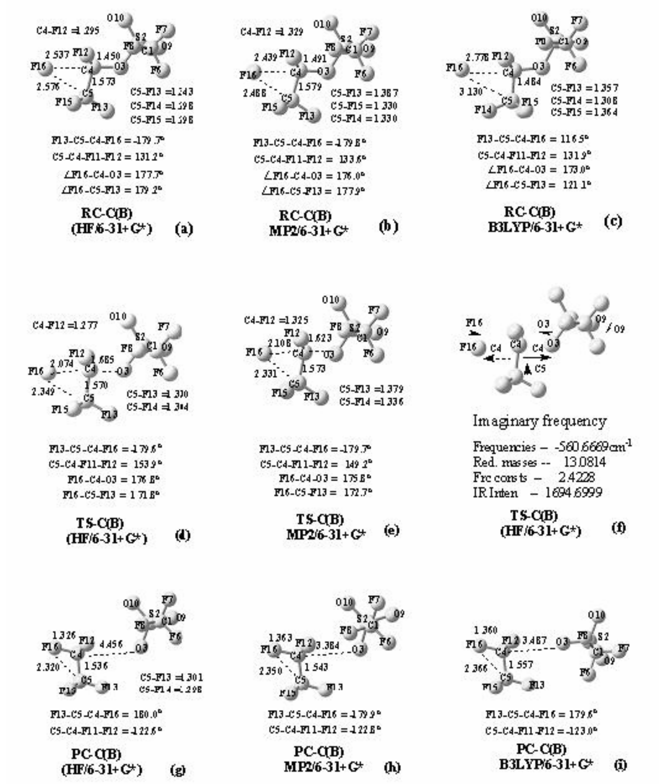

Figure 3.1.1: The Newman projections, looking down F12….F11, for RC-C(B) and TS-C(B) obtained from geometry optimization using HF, MP2 and B3LYP at 6-31+G* level (the bond length unit in Å).